Article

Scattering over Varying Amplification Grating

Er'el Granot *

Posted Date: 24 January 2024

doi: 10.20944/preprints202401.1699.v1

Keywords: Scattering Grating; amplification graing; Diffraction pattern

Article

Scattering Over Varying Amplification Grating

Er'el Granot

Department of Electrical and Electronics Engineering, Ariel Photonics Center, Ariel University, Ariel, Israel; erel@ariel.ac.il

Abstract: The scattering pattern from a narrow absorbing/amplifying grating is investigated. A simple model of a narrow amplifying grating is solved exactly numerically and approximately analytically for the regime where the beam's wavelength is much shorter than the grating's wavelength. The main results are: The incident angle divides the scattering pattern into two regimes: below and above the incident angles. The former regime has a weak dependence on the incident angle but has a strong dependence on the scattering one. In this regime, a new grating formula is derived. The opposite occurs in the latter regime, which is very sensitive to the incident angle, but has only weak dependence on the scattering angle. Consequently, at certain incident angles, all the scattering is concentrated in the first regime, i.e., all scattering angles are lower than the incident angle.

Keywords: scattering grating; amplification graing; diffraction pattern

1. Introduction

The periodicity of crystals and gratings exhibits universal scattering patterns, which are manifested by the well-known grating formula and grating's spectral resolution [1].

In general, the grating's scattering is much more complicated and it depends on the grating's material, profile, and grooving method[1-3]. In particular, plasmon excitations in the metal grating are responsible for anomalous scattering [4-6]. Moreover, it was found that even dielectric gratings exhibit anomalous scattering behavior [7,8]. These results were in clear contrast to the traditional belief that narrow dielectric gratings can have only a small effect on the incident light beam [9]. It was shown that even when the dielectric grating has weak modulation, the reflection coefficient can be very high [10-11]. The modulation can be either in the refraction index[12] or in the grating's grooves[7]. These results show that in principle the reflectance at specific incident angles can be arbitrarily close to 100%. It should be stressed that these angles (with 100% reflectance) have nothing to do with the grating formula.

This anomalous conduct is related to a specific case of Fano resonances [8,13-15]. Recently, it was shown that in theory perfect reflection (zero transmission) can occur for arbitrarily narrow dielectric grating layer [16]. The layer thickness can be arbitrarily narrow and the grating modulation amplitude can be arbitrarily low and still the effect of 100% reflectance occurs.

This conduct resembles a similar effect in Quantum Mechanics, where the transmission via an oscillating barrier can be suppressed completely at certain incoming particles' energies. Even though the quantum phenomenon was discovered after its optical equivalent, it was thoroughly investigated for both scattering scenarios [17-23] as well as for transition between adjacent quantum wells [24-26].

This effect occurs when the particle's energy approximately equals the oscillations' quanta. However, this is a relatively simple quantum system. When the system becomes more complex the dynamics are much less intuitive. In particular, it has been shown that if the oscillating potential is a well, which is located in an opaque barrier, then this system exhibits complex behavior. The current is extremely sensitive to the system's parameter, it can either increase substantially (activation and elevation) or almost vanish (complete suppression) [27-30].

When the barrier is absent this complex behavior vanishes. The reason is that the system's behavior is determined by the ratio between the oscillating potential's amplitude and the wavenumber in its vicinity. If this ratio is imaginary no complex behavior appears.

 doi:10.20944/preprints202401.1699.v1

The barrier's presence makes sure that the wavenumber is approximately real, and since the potential amplitude is real then the ratio is approximately real as well.

However, if the barrier is absent then the ratio can still be real provided the potential amplitude is imaginary. In that case, some of this complex behavior reappears.

While the physical application of an imaginary barrier is not entirely clear, the optical counterpart, i.e., imaginary wavenumber and imaginary refractive index are very common.

These conclusions can be applied to optical equivalent systems where the wavefunction is replaced with the electromagnetic field, and the oscillating potential is replaced with a spatial dielectric (grating as in Ref. [16] but for complex dielectric coefficient).

Then, similarly, the complex structure's dynamics can reappear by either putting the grating in a low index of refraction environment or by replacing the dielectric grating with an amplifying/absorbing one. In what follows we will focus on the latter: the scattering pattern of an amplifying/absorbing grating is going to be investigated.

Modulated amplification can be done by changing gradually the pumping over the grating causing a gradual change in the population inversion.

However, it is much simpler to create a uniform amplifying layer and attach to it a modulated absorber. If both layers are considerably narrower than the wavelength, then the two-layer system can be regarded as a single layer with modulated amplification/absorption.

2. The system under study

The system under study is a plane wave's scattering from a grating. This scenario is presented in Figure 1. A TE-polarized plane-wave beam hits an active grating at an incident angle θ. The grating is located on the x=0 plane. The gratings variations occur in the z-direction, in which case the electromagnetic Maxwell's wave equation can be written

$$\frac{\partial^2}{\partial x^2}\mathbf{E}+\frac{\partial^2}{\partial z^2}\mathbf{E}+k^2(x,z)\mathbf{E}=0 \tag{1}$$

where the electric field is polarized in the y-direction (TE polarization) $\mathbf{E}=\hat{y}E(x,z)$, and $k^2(x,z)$ satisfies

$$k^2(x,z)=k_0^2\{1+i\delta(x)d[\varepsilon''+\delta\varepsilon''\cos(Kz)]\} \tag{2}$$

where the grating's frequency is the reciprocal of the groove spacing Λ (the pitch), i.e.

$$K\equiv 2\pi/\Lambda\,. \tag{3}$$

In (2) we followed Ref.[16] and chose a delta function to represent the narrow grating's layer. As was explained in [16] (and references therein) a delta function is an excellent approximation for layers, which are shorter than the electromagnetic field's wavelength. To be more specific, a dielectric with the following properties $\varepsilon(x,y)=\begin{cases}\varepsilon_0(x,y) & 0<x<d\\ 0 & else\end{cases}$ where d is the narrow layer's thickness, can be approximated with great accuracy by $\delta(x)\int_0^d\varepsilon_0(x')dx'$. Since in what follows we focus on the limit of extremely narrow layers, this is an excellent approximation. Moreover, the validity of this approximation is improved when the incident angle increases, since the x-component of the beam's wavenumber decreases. We will see that it is easier to measure the effect in the large incident angle domain. When the incident angle approaches $\pi/2$ the approximation is accurate.

Preprints.org (www.preprints.org) | NOT PEER-REVIEWED | Posted: 24 January 2024 doi:10.20944/preprints202401.1699.v1

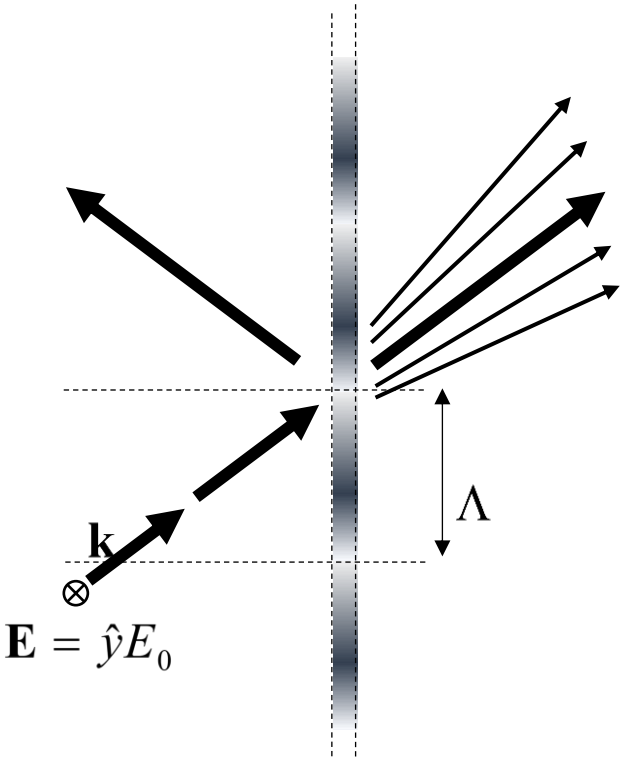

Figure 1. System schematic: diffraction by a thin grating. The arrows indicate the beam's scattering directions. The incident beam is polarized in the y-direction, and the wavenumber is $\mathbf{k} = k_0\left(\hat{x}\cos\theta + \hat{z}\sin\theta\right)$.

3. Exact Numerical Solution

Let θ be the incident angle, therefore the wavenumber is $\mathbf{k} = k_0\left(\hat{x}\cos\theta + \hat{z}\sin\theta\right)$ (see Figure 1), and the electromagnetic field can be written in all space as

$$E(x,z)/E_0 = \begin{cases} \exp\left[ik_0\left(x\cos\theta + z\sin\theta\right)\right] + \sum_n r_n \exp\left(-iq_n x + ip_n z\right) & x < 0 \\ \sum_n t_n \exp\left(iq_n x + ip_n z\right) & x > 0 \end{cases} \tag{4}$$

where $p_n \equiv k_0\sin\theta + Kn$ and $q_n \equiv \sqrt{k_0^2 - p_n^2} = k_0\sqrt{1-\left(\sin\theta + \lambda n/\Lambda\right)^2}$, i.e., $q_0 = k_0\cos\theta$ and $q_0 = k_0\cos\theta$. The boundary criterions on the grating requires

$$E\left(x=+0,z\right) = E\left(x=-0,z\right) \text{ and} \tag{5}$$

$$\frac{\partial}{\partial x}E(x,z)\bigg|_{x=+0} - \frac{\partial}{\partial x}E(x,z)\bigg|_{x=-0} = -id k_0^2\left[\varepsilon'' + \delta\varepsilon''\cos\left(Kz\right)\right]E\left(x=0,z\right)$$

and using the dimensionless parameters

$$s \equiv \lambda/\Lambda,\quad P_n \equiv p_n/k_0 = \sin\theta + ns\quad Q_n \equiv q_n/k_0 = \sqrt{1-\left(\sin\theta + ns\right)^2},\quad \alpha \equiv \tfrac{1}{2}dk_0\varepsilon'',\text{ and }\ \beta = dk_0\tfrac{1}{4}\delta\varepsilon'' \tag{6}$$

the problem reduces to the following difference equation

$$\left(Q_n + \alpha\right)t_n + \beta\left(t_{n+1} + t_{n-1}\right) = Q_0\delta\left(n\right) \tag{7}$$

which can be rewritten in a more compact matrix form

Preprints.org (www.preprints.org) | NOT PEER-REVIEWED | Posted: 24 January 2024 doi:10.20944/preprints202401.1699.v1

$$M_0 \cdot \mathbf{t} = \mathbf{v} \tag{8}$$

where

$$M_0 \equiv \begin{pmatrix} \ddots & \ddots & & & \\ \ddots & Q_{-1}+\alpha & \beta & & \\ & \beta & Q_0+\alpha & \beta & \\ & & \beta & Q_1+\alpha & \ddots \\ & & & \ddots & \ddots \end{pmatrix} \quad \mathbf{t} \equiv \begin{pmatrix} \vdots \\ t_{-1} \\ t_0 \\ t_1 \\ \vdots \end{pmatrix}, \text{ and } \quad \mathbf{v} \equiv \begin{pmatrix} \vdots \\ 0 \\ Q_0 \\ 0 \\ \vdots \end{pmatrix}. \tag{9}$$

The numerical solution of this set of equations is presented in Figure 2.

Eq.(7) illustrates the fact, which was mentioned in the introduction, that the dynamics is governed by the ratio between oscillations amplitude β and Q_n. When this ratio is imaginary (note that β is the imaginary part of the oscillations' amplitude), the spectrum cannot have a complex structure.

As can be seen from this figure, there are incident angles in which the transmission coefficient of the non-negative, i.e. $n \geq 0$, modes vanish. A small change in the incoming angle (~1.4% in Figure 2) reduces the positive modes' transmission probability from maximum value to zero. On the other hand, the incoming angle has a small effect on the negative modes (see Figure 2). Unlike the positive modes regime, where the differences between mode's amplitudes is small, on the negative regime, the spectrum consists of ridges and valleys. This spectrum structure and behavior is similar to the quantum system of Refs.[29].

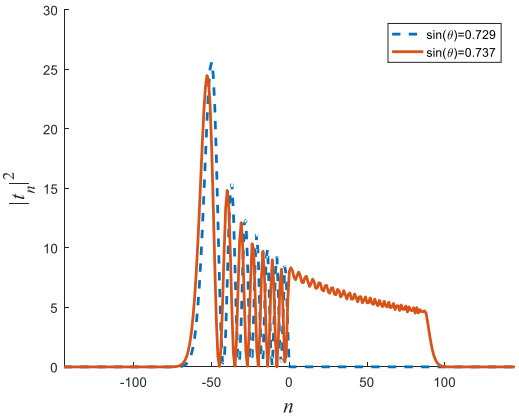

Figure 2. The transmission coefficient amplitude of the spectral modes for three different incoming angles. The parameters used in this simulation were: $\beta = 0.414$, $\alpha = 0$ $s = 0.003$ and 521 modes were used.

In Figure 3 the grating's scattering pattern is presented for these two incident angles. When the incident angle is $\sin\theta = 0.729$ then the e-m field is scattered only in the $\sin\theta_{sc} < 0.729$ angles. Nothing is scattered at angles, which exceed the incident angle $\sin\theta_{sc} > 0.729$. Below the incident angle, the e-m field is scattered at only specific angles.

On the other hand when the incident angle is $\sin\theta = 0.737$ the e-m is scattered at all angles even beyond the incident angle $\sin\theta_{sc} > 0.737$. Below the incident angle the scattering pattern is similar – in this regime, the e-m field is scattered at only specific angles.

Preprints.org (www.preprints.org) | NOT PEER-REVIEWED | Posted: 24 January 2024 doi:10.20944/preprints202401.1699.v1

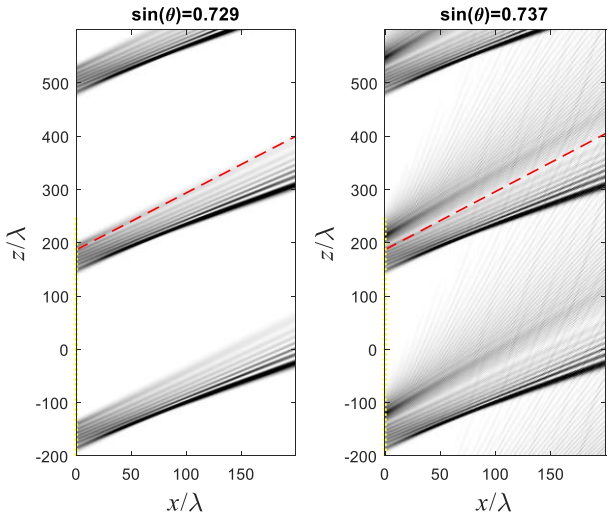

Figure 3. 2D image of the scattering pattern. The dashed line corresponds to direction of the incident beam. The darker the color the higher is the light intensity $|E(x,z)|^2$. The parameters in this case were: $s=0.003$, $\beta=0.414$, $\alpha=0$ and 521 modes were used.

Since all the $n\geq 0$ modes vanish simultaneously, one can focus on the central mode $n=0$. In Figure 4 the amplitude of the central mode is presented as a function of the incident angle. As can be seen, beyond a certain angle, the transmission coefficient vanishes for several angles.

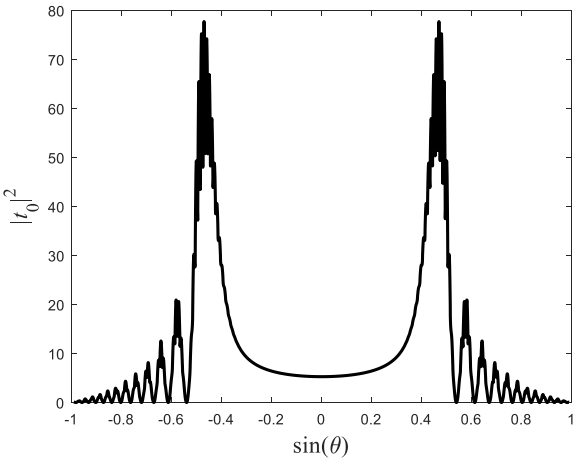

Figure 4. The transmission coefficient of the central, i.e., n=0, mode as a function of the incident angle. In this simulation $\beta=0.45$, $\alpha=0$, $s=0.01$ and 501 modes were used.

When the modulation depth β varies, so does the number of incident angles, in which the non-negative modes vanish. As can be seen in Figure 5, the larger the modulation depth, the larger the number of incident angles, in which the non-negative modes vanish.

Preprints.org (www.preprints.org) | NOT PEER-REVIEWED | Posted: 24 January 2024 doi:10.20944/preprints202401.1699.v1

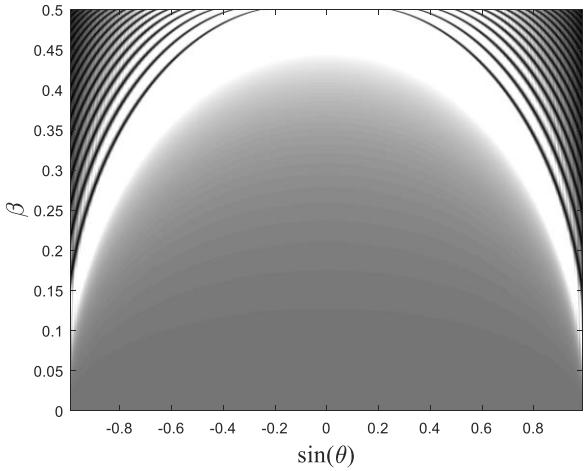

Figure 5. The transmission coefficient amplitude of the central mode as a function of the modulation depth and the incident angle. The darker the color the higher is the square of the coefficient amplitude. The same parameters of Figure 4. The parameters in this simulation were $s=0.01$, and $\alpha=0$ and 521 modes were used.

4. Approximate Analytical Derivation

The numerical studies shows that this effect occurs when the grating constant is considerably larger than the incident beam's wavelength. In this regime, Eq.(7) can be simplified to allow for analytical derivation. In this regime,

$$Q_n \equiv q_n / k_0 \cong \cos\theta - ns\tan\theta \tag{10}$$

which follows that Eq.(7) can be simplified to

$$\left(\frac{(\cos\theta+\alpha)}{\beta} - n\frac{s}{\beta}\tan\theta\right)t_n + (t_{n+1}+t_{n-1}) = \frac{Q_0}{\beta}\delta(n) \tag{11}$$

The solution of this difference equation can be solved with Bessel functions. Using Eq.(9.1.27) of Ref.[31]

$F_{\nu-1}(x)+F_{\nu+1}(x)=\frac{2\nu}{x}F_\nu(x)$ the solution of (11) can be written

$$t_n = \begin{cases} AJ_{-n+n_0}(u) & n<0 \\ CJ_{n-n_0}(u) & n>0 \end{cases} \tag{12}$$

where $n_0 \equiv \frac{(\cos\theta+\alpha)}{s\tan\theta}$, $u \equiv \frac{2\beta}{s\tan\theta}$, $J_n(u)$ are the Bessel functions of the first kind [31] and the coefficients A and C can be calculated by matching the solution and substituting the solution in (12), i.e.,

$$AJ_{n_0}(u) = CJ_{-n_0}(u), \text{ and } \quad \frac{s}{\beta}\tan\theta(n_0)CJ_{-n_0}(u) + \left(CJ_{1-n_0}(u) + AJ_{1+n_0}(u)\right) = \frac{Q_0}{\beta}.$$

The solution therefore reads

$$A = \frac{\frac{Q_0}{\beta}J_{-n_0}(u)}{\frac{s}{\beta}\tan\theta(n_0)J_{-n_0}(u)J_{n_0}(u) + \left(J_{n_0}(u)J_{1-n_0}(u) + J_{-n_0}(u)J_{1+n_0}(u)\right)} \tag{13}$$

 doi:10.20944/preprints202401.1699.v1

$$C=\frac{\frac{Q_0}{\beta}J_{n_0}(u)}{\frac{s}{\beta}\tan\theta(n_0)J_{-n_0}(u)J_{n_0}(u)+\left(J_{n_0}(u)J_{1-n_0}(u)+J_{-n_0}(u)J_{1+n_0}(u)\right)} \tag{14}$$

Now we have an approximate solution of the entire spatial spectrum, from which two main results can be derived: (A) the incident angles in which the scattered e-m is bounded to the lower angles, i.e., the scattered angles are lower than the incident angles. (B) The scattering angles below the incident one.

5. Calculating the incident angles for which scattering is bounded

From (12) and (14) if follows that suppression of high angles scattering occurs for $C=0$, i.e. for

$$J_{n_0}(u)=0 \tag{15}$$

and in which case all the $n\geq 0$ modes vanish as well.

Since this approximation was derived for the limit of $s<<1$ then both relations $\frac{2\beta}{s\tan\theta}>>1$ and $n_0>>1$ hold. Therefore, using Eq.(9.3.3) of Ref.[31],

$$J_\nu(\nu\sec B)\cong\sqrt{\frac{2}{\pi\nu\tan B}}\cos\left[\nu(\tan B-B)-\pi/4\right] \tag{16}$$

where in this case $B\equiv\arccos\left(\frac{\cos\theta+\alpha}{2\beta}\right)$ and $\nu\equiv n_0$. (17)

For a solution, in which the argument of the cosine function of (16) is small whilst still $s<<1$, the parameter B must be accordingly small. Therefore, we seek a solution around

$$\cos\theta\cong 2\beta-\alpha, \tag{18}$$

in which case, (15) and (16) yields

$$n_0B^3/3=\left(m+\tfrac{3}{4}\right)\pi \tag{19}$$

Solving (19) for β, we finally obtain the condition for high angles suppression

$$\beta\cong\frac{(\cos\theta+\alpha)}{2}\left[1+\frac{1}{2}\left[3\frac{s\tan\theta}{(\cos\theta+\alpha)}\left(m+\frac{3}{4}\right)\pi\right]^{2/3}\right] \tag{20}$$

or equivalently, one can find the incident angles θ_m for which high angle scattering does not occur

$$\cos\theta_m\cong 2\beta\left[1+\frac{1}{2}\left[3\frac{s}{2\beta}\sqrt{(2\beta-\alpha)^{-2}-1}\left(m+\frac{3}{4}\right)\pi\right]^{2/3}\right]^{-1}-\alpha \tag{21}$$

In Figure 6 the approximation (20) is plotted on top of the exact numerical simulation (Figure 5). As can be seen, this approximation shows high agreement with numerical results.

 doi:10.20944/preprints202401.1699.v1

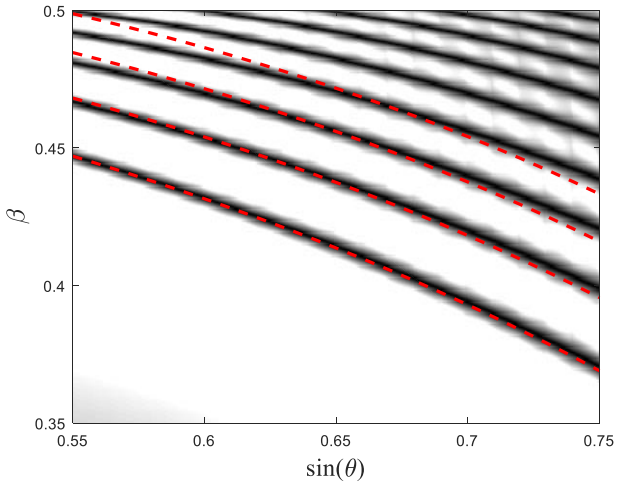

Figure 6. Zoom in of Figure 5. The dashed curves represents the approximation (20) for four integers m.

6. Scattering Angles

The scattered beam takes the following form

$$E(x,z)/E_0 = \sum_n t_n \exp(iq_n x + ip_n z) = \sum_n AJ_{-n+n_0}\left(\frac{2\beta}{s\tan\theta}\right)\exp\left(ik_0\left(\sqrt{1-(\sin\theta+ns)^2}\,x+(\sin\theta+ns)z\right)\right) \tag{22}$$

where A is the constant (13).

To calculate the scattering angles, one can use the fact that $s<<1$. In this case the summation can be approximated by an integral

$$E(x,z)/E_0 \cong s^{-1}A\int d\eta J_{(\eta_0-\eta)/s}\left(\frac{2\beta}{s\tan\theta}\right)\exp\left(ik_0\left(\sqrt{1-(\sin\theta+\eta)^2}\,x+(\sin\theta+\eta)z\right)\right) \tag{23}$$

Using the method of stationary phase approximation, this integral can be evaluated at

$$\sin\theta_{sc} - \sin\theta = \eta \tag{24}$$

Note that (24) is the classical grating formula.

Therefore, the scattering amplitude at the scattering angle θ_{sc} is approximately

$$\left|AJ_{(\eta_0-(\sin\theta_{sc}-\sin\theta))/s}\left(\frac{2\beta}{s\tan\theta}\right)\right|^2 \tag{25}$$

Again, since $s<<1$ one can use Eq.(9.3.3) of Ref.[31], in which case

$$B \cong \sqrt{2\left(1-\frac{(\cos\theta+\alpha)-ns\tan\theta}{2\beta}\right)} \tag{26}$$

the angles which yields the maximum value of (25) must satisfy

$$n_0 B^3/3 - \pi/4 = (m\pi) \tag{27}$$

 doi:10.20944/preprints202401.1699.v1

Substituting (26) in (27) and solving the angle, while keeping in mind that $\sin\theta_{out}-\sin\theta=\eta$ one finally get the grating formula

$$\left(\sin\theta_{out}^{m}-\sin\theta\right)\cong\left[\beta\left\{\left[\frac{3\pi}{n_0}\left(m+\tfrac{1}{4}\right)\right]^{2/3}-2\right\}+\left(\cos\theta+\alpha\right)\right]\cot\theta \tag{28}$$

As can be seen in Figure 7 the scattered angles θ_{out}^{m} for $m=0,1$, and 2 shows high agreement with the approximation (28). It should be stressed that the grating formula (28) appears on top of the classical one (24).

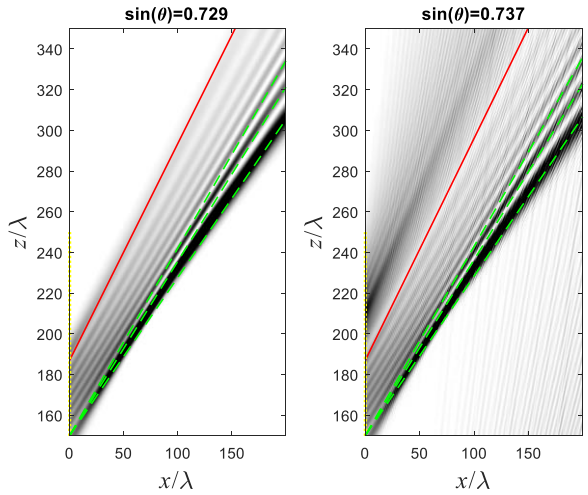

Figure 7. Zoom in of Figure 3 with the same parameters. The solid line represents the incident beam's direction, and the dashed lines represents the scattered directions according to the approximation of the grating's formula(28).

7. Physical Realization

The realization of this grating requires simultaneous changes in both the real and imaginary components of the refractive index, however, they do not change in the same manner.

To simplify the model, the harmonic change occurs in the imaginary component of the dielectric constant $\delta\varepsilon''\cos(Kz)$. Therefore, the real and imaginary parts of the refraction index are

$$\Im n=2^{-1/2}\delta\varepsilon''\cos(Kz)/\sqrt{1+\sqrt{1+\left(\delta\varepsilon''\cos(Kz)\right)^2}} \tag{29}$$

$$\Re n=2^{-1/2}\sqrt{1+\sqrt{1+\left(\delta\varepsilon''\cos(Kz)\right)^2}} \tag{30}$$

These components are plotted in Figure 8 for $\delta\varepsilon''=5$. As can be seen, for this value, the real part of the refractive index changes between 1 and 1.7, while the imaginary part varies between -1.5 to +1.5. Then, if the layer thickness is $d/\lambda\cong0.03$ then $\beta=dk_0\frac{1}{4}\delta\varepsilon''\cong0.24$, which is sufficient to measure several angles which shows this effect (according to Figure 5). It should be noted that if we seek the effect at high, i.e., grazing, angles, the layers width can be increased substantially, while keeping the narrow layer approximation still. In this case multiple angles should be detected. Moreover, Most of this work concentrated, for simplicity, on the $\alpha=0$ scenario, however, by varying α the effect will appear even for very weak β, in which case, it will be easier to measure the effect. Nevertheless, a full study of this effect for different values of α and different modulations is beyond the scope of this paper.

 doi:10.20944/preprints202401.1699.v1

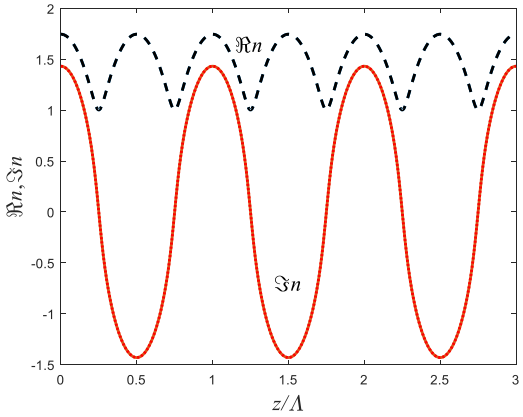

Figure 8. The real (dashed curve) and imaginary (solid curve) parts of the refraction index along the grating (z-axis) according to (30) and (29) respectively.

8. Summary

The scattering from an active grating layer was analyzed. In this model, the imaginary component of the dielectric coefficient varies harmonically. The grating's layer width is shorter than the optical beam wavelength, while the grating's wavelength is longer than the beam's wavelength. A new grating formula is formulated, which is the profile on top of the classical grating formula. An approximate analytical expression for this formula was derived. Besides the scattering orders, a special scattering pattern appears for certain incident angles.

It was found that in some cases, the scattering angles θ_{out} cannot exceed the incident angle θ, i.e., for specific $\theta = \theta_m$ the scattered angles obey $\theta_{out} \le \theta$.

References

1. C. H. Wilcox, "Scattering Theory for Diffraction Gratings", Springer-Verlag, (New-York 1984)
2. E. Popov (Ed.), "Gratings: Theory and Numeric Applications", Presses universitaires de Provence (PUP 2012)
3. C. Palmer and E. Loewen, "Diffraction Grating Handbook", Newport Corporation 2005
4. J.R. Piper, and S. Fan, "Total absorption in a Graphene Monolayer in the Optical Regime by Critical Coupling with a Photonic Crystal Guided Resonance", ACS Photonics, 1, 4, 347–353 (2014)
5. M. C. Hutley and D. Maystre, "Total absorption of light by a diffraction grating," Opt. Commun. 19, 431-436 (1976)
6. M. J. Jory, P. S. Vukusic, and J. R. Sambles, "Development of a prototype gas sensor using surface plasmon resonance on gratings," Sens. Actuators B 17, 203-209 (1994)
7. L. Mashev and E. Popov, "Zero order anomaly of dielectric coated gratings", Optics. Commun. 55, 377 (1985)
8. E. Popov, L. Mashev and D. Maystre, "Theoretical study of the anomalies of coated dielectric gratings", Optica Acta, 33, 607-619 (1986)
9. C.B. Burckhardt, "Efficiency of a Dielectric Grating", J. Opt. Soc. Am. 57, 601 (1967)
10. S. Tibuleac and R. Magnusson, "Reflection and Transmission guided-mode resonance filters", J. Opt. Soc. Am. A 14, 1617(1997)
11. S. Tibuleac and R. Magnusson,"Narrow-linewidth bandpass filters with diffractive thin-film layers", Opt. Lett. 26, 584 (2001)
12. S.S. Wang, R. Magnusson, J.S. Bagby, and M.G. Moharam, "Guided-mode resonance in planar dielectric-layer diffraction gratings", J. Opt. Soc. Am. A 7, 1470 (1990)
13. U. Fano, "The theory of anomalous diffraction gratings and of quasi-stationary waves on metallic surfaces (Sommerfield's waves)," J. Opt. Soc. Am. 31, 213–222 (1941).
14. A. Hessel and A. A. Oliner, "A new theory of Wood's anomalies on optical gratings," Appl. Opt. 4, 1275–1297 (1965).
15. S. Fan, W. Suh, and J. D. Joannopoulos, "Temporal coupled-mode theory for Fano resonant mode in optical resonators," J. Opt. Soc. Am. A 20(3), 569-572 (2003).
16. E. Granot, "Derivation of analytical expressions for anomalous reflection in the limit of zero thickness and weakly modulated dielectric grating," J. Opt. Soc. Am. A 39, 2205-2213 (2022)

17. E. Cota, J.V. Jose, F. Rojas, "Electronic transmission through time-periodic oscillating barriers" Nanostructured Materials, 3, 349 (1993)
18. P.F. Bagwell, R.K. Lake, "Resonances in transmission through an oscillating barrier", Phys.Rev.B, 46, 15329(1992)
19. W. Li and L. E. Reichl, "Floquet scattering through a time-periodic potential", Phys. Rev. B, 60, 15732 (1999)
20. D.S. Saraga, M. Sassoli-de-Bianchi, " On the One-Dimensional Scattering by Time-Periodic Potentials: General Theory and Application to Two Specific Models", Helv. Phys. Acta, 70, 751(1997).
21. D. F. Martinez, L. E. Reichl, " Transmission Properties of the oscillating delta-function potential" Phys. Rev. B, 64 (2001)
22. D. L. Haavig and R. Reifenberger, "Dynamic transmission and reflection phenomena for a time-dependent rectangular potential", Phys. Rev. B 26, 6408 (1982)
23. W. Cai, P. Hu, T. F. Zheng, and B.Yudanin, "Resonance of the one-dimensional electron transmission above a quantum well with dissipation" Phys. Rev. B 41, 3513 (1990)
24. Y. Kayanuma, Role of phase coherence in the transition dynamics of a periodically driven two-level system, Phys. Rev. A, **50**, 843, (1994).
25. Y. Kayanuma, Stokes phase and geometrical phase in a driven two-level system, Phys. Rev. A, **55**, 2495, (1997).
26. A. del Campo, G. Garcia-Calderon, J. G. Muga, Quantum transients, Phys.Rep. 476, 1 (2009),
27. M. Y. Azbel, Eigenstate assisted activation, Phys. Rev. Lett, **68**, 98, (1992).
28. G. Zangwill and E. Granot, Eigenstate suppressed activation, Physica B: Condensed Matter, **461**, 140, (2015).
29. E. Granot, Selected elevation in quantum tunneling, Europhys. Lett. , **61**, 817, (2003).
30. E. Granot, The Tunneling Current through Oscillating Resonance and the Sisyphus Effect, Adv. Cond. Matter Phys. **2017**, 2435857, (2017).
31. M. Abramowitz and A. Stegun, *Handbook of Mathematical Functions* (Dover Publications, New York, 1965).